

Design and simulation of DBR lasers with extended modulation bandwidth exploiting photon-photon resonance effects

Paolo Bardella, Ivo Montrosset
 Dipartimento di Elettronica e Telecomunicazioni
 Politecnico di Torino, Torino, Italy
 ivo.montrosset@polito.it

Abstract— In high-speed laser devices the occurrence of a photon-photon resonance increases the modulation bandwidth substantially. In this paper our attention is focused on the design of DBR lasers in which this effect is exploited.

Keywords - DBR lasers, photon-photon resonance, detuned loading, extended modulation, time-domain simulation

I. INTRODUCTION

In conventional high-speed laser devices the modulation response is largely determined by the carrier-photon resonance (CPR). However, the occurrence of a photon-photon resonance (PPR) can increase the -3dB modulation bandwidth substantially. In this paper our attention is focused on the design of a DBR cavity in which the PPR frequency is fixed by the design procedure. The PPR has been observed in distributed Bragg reflector (DBR) laser diodes [1,2], in coupled-cavity-injection-grating (CCIG) lasers [3,5], and in passive-feedback lasers [6,7], but a thorough explanation to achieve this operation condition also in simple DBR lasers has not been presented [8,9]. The design procedure for DBR cavity laser is here identified; the small and large signal modulation results presented support the correctness and accuracy of the proposed design procedure.

II. DESIGN PROCEDURE

In this paper we present a design procedure for a simple DBR cavity that allows obtaining with a good accuracy a PPR effect at the desired frequency. This is very important in practical applications because the gap between the traditional CPR and the PPR in the small signal intensity modulation (IM) response should be filled by the contribution of the two effects in order to avoid unwanted reduction of the device modulation response (Fig.1).

For this reason the CPR response should be as wide as possible respect to the PPR frequency; this can be obtained e.g. by operating the laser in the so called detuned loading condition [8]. When the laser is operating in this condition a particular attention must be paid to avoid mode competition between the lasing mode (at longer wavelength respect to the Bragg peak) and the cavity mode on the other side of the stop band. There-

The work reported in this paper has been carried out within the EU FP7 project “Development of low-cost technologies for the fabrication of high-performance telecommunication lasers” (DeLight) under grant agreement n° 224366.

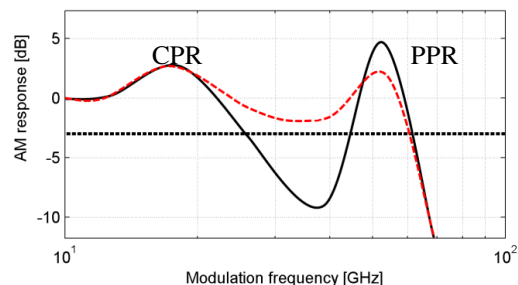


Figure 1. Example of IM responses. The PPR peak is not sufficient to obtain an efficient extension of the modulation bandwidth if a strong gap is present between CPR and PPR (black continuous line): the CPR should be wide enough to flatten the IM response (red dashed line).

fore the cavity should be designed in such a way that the Free Spectral Range of the cavity inside the grating stop band is comparable to the separation between the first two minima of the grating reflectivity function around the Bragg wavelength.

Once this condition is fulfilled, and enhanced CPR modulation bandwidth can be obtained without the risk of mode competition, we can then enforce the second condition on the PPR frequency, which corresponds to the separation between the lasing mode and the side mode (PPR mode): we impose this side mode to be on the first side lobe of the reflectivity function as shown in the example of the Round Trip gain and phase function reported in Fig.2.

Using the simple resonance equation condition for the detuned lasing mode and the corresponding side mode generating the PPR one can relate the following cavity parameters: active

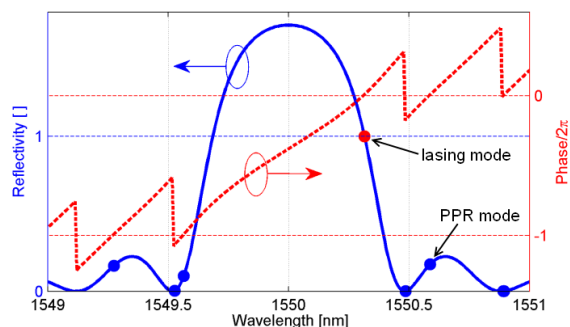


Figure 2. Round Trip Gain (RTG, blue curve) and phase (red curve) function at threshold for a DBR cavity. The squared red point represents the lasing mode; the blue markers indicate cavity modes below threshold.

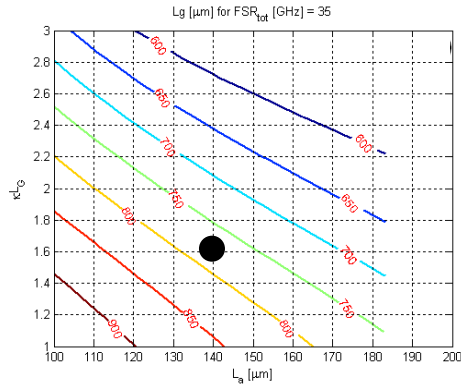


Figure 3. Values of L_G (in μm) required to obtain a 35GHz PPR, as a function of L_A and κL_G . The circular black marker highlights the structure considered in the Time-Domain analysis.

and grating section lengths (L_A , L_G), grating coupling coefficient (κ) and PPR frequency.

The results are reported in the map in Fig. 3, obtained for a chosen PPR frequency of 35GHz between the lasing mode operating at the maximum detuned loading condition and the PPR mode located in the first side mode of the reflectivity function: in the plane ($L_A - \kappa L_G$) we present the values of L_G satisfying the requested PPR frequency.

III. SIMULATION RESULTS

For the device indicated by the marker in Fig. 3, whose characteristic parameters are illustrated in Table I, we computed the small and the wide digital signal modulation response using our Finite-Difference Travelling-Wave program [10].

In Fig. 4 a color map of the normalized small signal modulation response [11] is presented; the modulation frequency is reported in the abscissa while in the ordinates the lasing mode position respect to the Bragg frequency is varied changing the phase ϕ_A of the cleaved facet mirror reflectivity at the active region side. A similar tuning effect can be obtained changing the current injected in the Bragg grating.

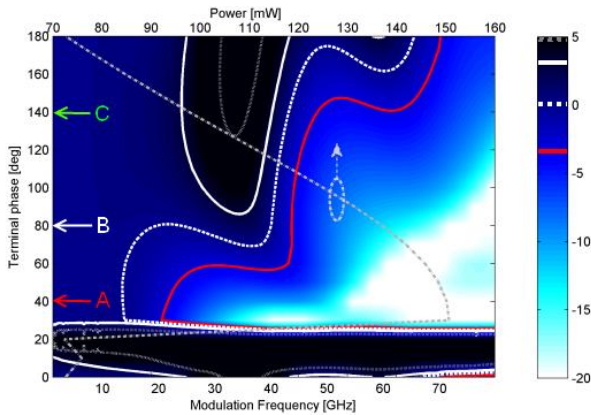


Figure 4. Modulation map of the considered device, obtained at the bias current of 200mA, as a function of ϕ_A . The red continuous line indicates the -3dB modulation response level, while the white dashed, continuous and dotted lines represent the 0dB, +3dB and +5dB modulation response levels respectively; the gray dash-dotted line refers to the output power whose values are reported on the axis in the upper border of the figure. The 3 values of the ϕ_A parameter considered for the large signal analysis are indicated with arrows

TABLE I. PARAMETERS USED IN THE TIME-DOMAIN ANALYSIS

Parameters description and symbols [11]	Values
Active region length, L_A	140 μm
Bragg grating region length, L_G	780 μm
Grating coupling coefficient, κ	21 cm^{-1}
Transversal optical confinement factor, Γ_{xy}	0.15
Differential gain, a	10 10^{-16}cm^2
Transparent carrier density, N_{tr}	10 ¹⁸ cm^{-3}
Active region intrinsic losses, $\alpha_{i,A}$	10 cm^{-1}
Bragg grating region intrinsic losses, $\alpha_{i,G}$	5 cm^{-1}
Linewidth enhancement factor, α	3
Gain compression factor, ϵ	5 10^{-17}cm^3

Evidence of PPR around 35GHz is quite clear from this modulation map. The dark strip the IM color map in the range 0° – 30° corresponds to a self pulsation condition [10].

Large signal modulations were calculated for the three values of terminal phase indicated in Fig 4 using a NRZ PRBS signal at different modulation bit rates. The choice was done to compare the cases without (case A) and with (case B) PPR effect and to see the limitations to the maximum achievable large signal modulation introduced by a too pronounced modulation response peak in the small signal response (case C).

The corresponding eye diagrams are presented in Fig. 5. As shown from the 40Gb/s signal modulation the response with a high resonance peak (case C) is strongly reducing the eye opening and the small signal modulation bandwidth represents in this case an upper limit for the achievable large signal modulation. In the other two cases (A, B) the large signal modulation bandwidth can be extended significantly beyond the -3dB modulation band (up to 40Gb/s and 60Gb/s, respectively).

IV. CONCLUSIONS

A novel procedure to design DBR lasers with extended modulation bandwidth has been presented and validated by large signal digital modulation simulations. The results show that in some conditions it is possible to extend significantly the -3dB modulation bandwidth and also the transmission bit rate.

REFERENCES

- [1] O. Kjebon et al., Electron. Lett., 33, pp. 488–489, 1997.
- [2] L. Bach et al., IEEE Photon. Technol. Lett., 16, pp. 18–20, 2004.
- [3] W. Kaiser et al., IEEE Photon. Technol. Lett., 16, pp. 1997–1999, 2004.
- [4] F. Gerschütz et al., Opt. Express, 16, pp. 5596–5601, 2008.
- [5] M. Vallone et al., IEEE J. Quantum. Electron., 47, pp. 1269–1276, 2011.
- [6] M. Radziunas et al., IEEE J. Sel. Top. Quantum Electron., 13, pp. 136–142, 2007.
- [7] U. Troppenz et al., ECOC 2009, 20–24 September, Vienna, 2009.
- [8] U. Feiste, IEEE J. Quantum Electron., 34, pp. 2371–2379, 1998.
- [9] G. Morthier et al. IEEE J. Quantum Electron., 36, pp. 1468–1475, 2000.
- [10] L.A. Coldren, S.W. Corzine, Diode Lasers and Photonic Integrated Circuits, Wiley, New York, 1995.
- [11] P. Bardella, I. Montrosset, IEEE J. Sel. Top. Quantum Electron., 11, pp. 361–366, 2005.

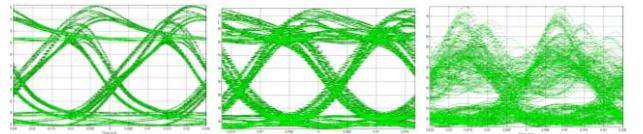


Figure 5. (left) 40Gb/s eye diagram computed for case A; extinction ratio (ER) = 6dB. (center) 60Gb/s eye diagram computed for case B; ER = 4.5dB. (right) 40Gb/s eye diagram computed for case C.